Optical and ESR study of Nd:YAG transparent polycrystalline ceramics

Weinan Gao (高伟男), Yu Shen (申 玉), Yong Bo (薄 勇), Wenping Zhang (张文平)*, Yong Bi (毕 勇), and Zuyan Xu (许祖彦)

Research Center for Applied Laser, Technical Institute of Physics and Chemistry, Chinese Academy of Sciences, Beijing 100190, China

**corresponding author: zwp@mail.ipc.ac.cn*

Received December 16, 2016; accepted January 24, 2017; posted online February 23, 2017

In this Letter, ceramic Nd:YAG is charactrizeby electron spin resonance (ESR) measurements. The ESR results indicate that the polycrystalline ceramic Nd:YAG has barely native defects and impurity ions localization defects, compared to an Nd:YAG crystal with the same Nd doping concentration, due to its density structure by sintering in a vacuum pure raw material and additives during the fabrication. It may conclude that the high quality ceramic Nd:YAG may have greater ability on optical characteristic, mechanical performance, and laser damage than that of the crystals, which is a promising candidate to use on laser diode-pumped solid-state lasers.

OCIS codes: 160.3380, 140.3580.
doi: 10.3788/COL201715.051601.

Polycrystalline transparent ceramic Nd:YAG laser material enables new possibilities as a new laser gain medium according to its favorable characteristics such as higher doping concentration, multifunction samples, mass production, large size, and low cost[1–3]. Specifically, high-quality ceramic Nd:YAG possesses a lower optical scattering loss, higher mechanical strength, and a larger laser damage threshold than that obtained in a single Nd crystal[4–7], and ceramic Nd:YAG has shown intriguing potential as high power laser platforms[8–11]. The previous investigations on transparent ceramic Nd:YAG laser materials were focused on optical and laser property comparison to crystalline Nd:YAG materials[12]. While micro-defect detection for the two materials has not been available up to now, it is possibly an important factor for their optical and laser characteristics.

To our knowledge, electron spin resonance (ESR) is an effective method to obtain the detailed information about native defects and impurities in the crystal; we intend to use this technological procedure to study defects that may be caused by raw material contamination and also the technology of crystal growth. A ceramic cylindrical Nd:YAG rod is selected to test the optical and laser characteristics. Then, we discuss the possible reasons for the defect formation indicated by the ESR results.

For laser device design, spectroscopic properties of the laser material are important factors. The absorption spectra were measured using an Excalibur 3100 beam spectrophotometer. The Excalibur 3100 compares the transmission of two beams. One beam acts as a reference while the other beam passes through the sample. The comparison of the beams reveals the absorption coefficient at a given wavelength. The instrument scans through many wavelengths to generate the absorption spectrum of the sample being tested.

Consider the application to a solid state laser in around 1 μm of polycrystalline ceramic. The absorption coefficient is measured for a wavelength range of 780–830 nm and is shown in Fig. 1. From Fig. 1, we can see the typical absorption peaks of 1% Nd-doped Nd:YAG ceramic, such as 795, 808, 812 nm, etc. The maximum absorption peak at 808 nm wavelength can be typically used for diode pumping, with the absorption coefficient proportional to the Nd^{3+} doping level, as expected.

Figure 2 shows the emission spectrum measured at room temperature for a 1% Nd-doped Nd:YAG ceramic. Fluorescence lifetime has also been measured for a ceramic crystal, about 246 μs. The measured fluorescence lifetime is a little higher than for other measurements, from the literature[13,14]. The different results of lifetimes may be due to the nonuniformities in the dopant distribution.

To quantify the laser characteristics, a short flat-to-flat cavity is designed. One ceramic cylindrical Nd:YAG rod is used in this experiment (1.0 at. % Nd^{3+}-doped, Φ3 mm × 70 mm), provided by Shanghai Institute of

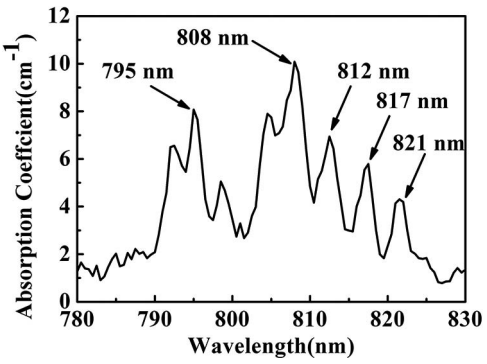

Fig. 1. Absorbance spectra as a function of wavelength for a 1% Nd-doped Nd:YAG ceramic.

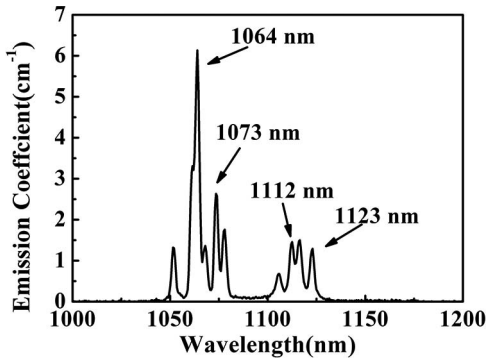

Fig. 2. Emission spectrum as measured for a 1% Nd-doped Nd:YAG ceramic from the F900 instrument.

Ceramics, Chinese Academy of Sciences. The experimental setup for the composite ceramic Nd:YAG laser rod setup is shown in Fig. 3. There were five quasi-continuous wave diode arrays in the laser module and each diode array operating at a frequency of 1000 Hz and a pulse duration of 200 μs at a wavelength of 808 nm, and the total pump power was 210 W. The laser diode (LD) is stabilized to an individual water cooling module at 25°C for emission wavelength tuning to meet maximum absorption at the wavelength of 808 nm in the laser rod. M1 and M2 are two flat mirrors, which are rear mirror and output coupler (OC), respectively. M1 is high reflection coated with reflectivity $R > 99.5\%$ at 1 μm, and M2 is coated with transmission $T = 40\%$ around 1 μm.

The output power of the ceramic rod Nd:YAG laser at 1 μm is measured with a power meter (Ophir F300A-SH) in Fig. 4. We achieve a maximum output power of 54.6 W

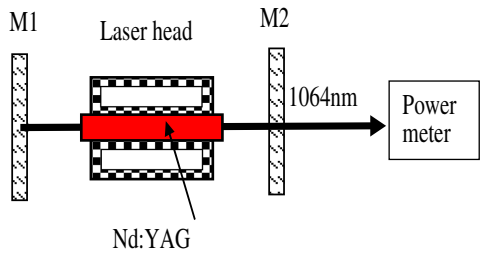

Fig. 3. Experiment setup of a solid ceramic Nd:YAG laser.

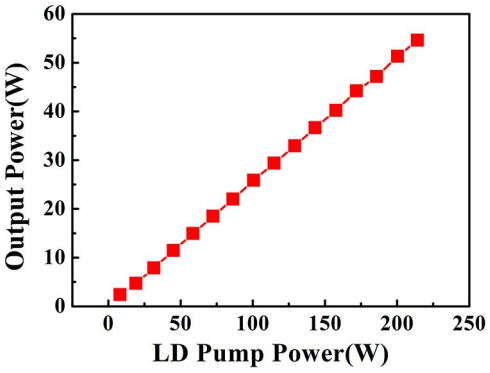

Fig. 4. Output power of the ceramic Nd:YAG.

with the optical to optical efficiency of about 25.5%. The micro defects, such as native defects and impurity defects, generated during the as-grown process are detected and quantitatively analyzed in this part by ESR measurements. For comparison, the ESR spectra of polycrystalline ceramic and crystal Nd:YAG are shown in Fig. 5 using a Bruker E500. The general garnet structure (YAG) has a space group of Ia3d with a chemical formula of $A_3B'_2B'_3O_{12}$[15]. The A site is usually occupied by a rare-earth ion such as Y^{3+}; the B′ and B″ can be occupied by the same transition elements such as Al^{3+} in YAG or Ga^{3+} in GGG. Polycrystalline ceramic and crystal Nd:YAG are both formulated by a YAG structure with doped Nd^{3+} ions of the same concentration.

The ESR spectroscopy method can show valuable information about the details of microstructure, lattice location, charge state of point defects, and impurities for studying the materials with nuclear magnetic resonance. According to Pauli's exclusion principle, every electron has two energy levels with $m_s = 1/2$ (parallel) and $m_s = -1/2$ (nonparallel). Under the condition of an external magnetic field, a collection of paramagnetic centers, such as free radicals, is exposed to microwaves at an external magnetic field. The gap between the parallel and nonparallel energy states is widened until it matches the energy of the microwaves. There are more electrons in the lower state due to the Maxwell–Boltzmann distribution that is monitored and converted into a spectrum. The ESR technique can be used to quantitatively testify the initial defects in numbers.

According to Fig. 5, we note that there are very different ESR results for ceramic and crystal3. The ESR spectra of curve (b) shows the presence of several types of paramagnetic ions that curve (a) does not observe, and also the intensity of the crystal Nd:YAG is higher than that of the ceramic. In order to investigate in more detail the intensity difference in the YAG crystal and ceramic as demonstrated in the ESR results, we discuss the possibile effect on the laser characteristics in the two materials. The same paramagnetic positions of Nd^{3+} for both the Nd:YAG crystal and ceramic are shown at 2300 and 2950 Gauss, respectively. The intensity of free Nd^{3+} for a crystal has a higher intensity than ceramic at the same

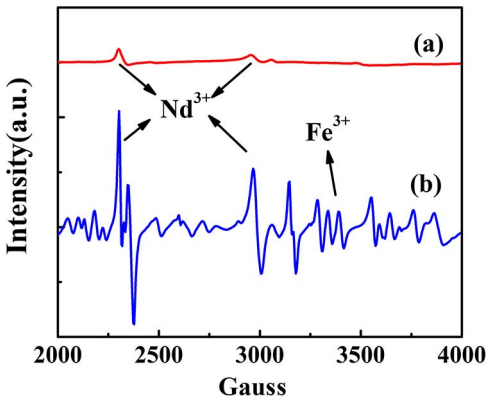

Fig. 5. ESR spectra of the Nd:YAG (a) polycrystalline ceramic and (b) crystals at room temperature.

magnetic field. For this investigation of the different ESR results, the higher intensity implies an existence of more free Nd^{3+} electrons in the Nd:YAG crystal lattice than that of the ceramic and may affect the laser performance characteristics. During the laser operation process the localization of free Nd^{3+} ions may capture the pumped light and decrease the pumped efficiency, cause a loss of transmittance and the transmission may rise. On the contrary, the less intensity for ceramic indicates that the Nd^{3+} ions may be used in the YAG lattice with a high utilization. It may be caused by two reasons: one possible reason is that ceramic is used with additives such as MgO and SiO_2. Mg^{2+} ions, as divalent impurities, may be located in any caption site to form acceptor defects. Oxygen vacancies, as donor defects, can compensate for the generated acceptor defects to form neutral aggregates. Si^{4+} ions, as tetravalent impurities, may be well-distributed placed at the Al site. Therefore, Nd^{3+} ions are placed at the Y site in the lattice and the surplus Nd^{3+} ions can accompany caption vacancies, which may favor improving uniformity and the Nd^{3+} doping concentration. The different ESR results of two materials with doping of the same Nd^{3+} concentration show that the ceramic has a potential ability to apply to higher-power output laser design.

Moreover, the ESR spectra of curve (b) shows the presence of several types of paramagnetic ions that curve (a) does not observe. It may be caused by other types of impurity ions. The additional paramagnetic positions may have a complex effect on the characteristics of laser performance. Based on the g-factor analysis, the resonance positions from 2000–2200 Gauss may be denoted as Pt or Mo[16], depending on the different crucible. The Czochralski technique of Nd:YAG crystal growth in a molybdenum or platinum crucible possibly contributes to Mo or Pt ion contamination in the crystal Nd:YAG. Further research is required, such as lower measurement temperature, to analyze the detailed information. Another typical resonance positios at 3550 Gauss of curve (b) may be assigned as Fe^{3+} ions. Fe^{3+} impurity may mainly come from the evaporation of impurities such as ZrO_2, which contains Fe_2O_3 impurity[17]. On the other hand, in curve (a) of Fig. 5 there is barely any Fe^{3+} ion locations because the ceramic Nd:YAG is fabricated by more pure raw materials and sintering in a vacuum. More detailed study is required to clarify the other unconfirmed paramagnetic regions and the influence on optical and laser characteristics.

In conclusion, the spectroscopic and laser performance of polycrystalline ceramic Nd:YAG is performed and discussed. Specifically, we use the ESR measurement method to quantitatively analyze the initial defects. The results of the ESR spectra indicate that the transparent ceramic Nd:YAG may have a greater ability to obtain a density structure with less initial defects because of the method of vacuum sintering, pure raw material, and additives than that of the crystal Nd:YAG. The surprising characteristics of high quality with better density structure, less initial defects, and more Nd^{3+} doping concentration about the ceramic laser materials[18] may demonstrate its potential reliability for additional applications such as some hardness environments and high-power LD-pumped solid-state lasers.

Recently, in the YAG lattice, antisite defects are the primary crucial influence on the carrier transportation and other optical prosperities. The antisites, whether Al^{3+} ions are placed at the Y^{3+} site (Al_Y) or Y^{3+} ion, are placed at the Al site (Y_{Al}) depend on the excess of Y or Al. An antisite substitution Y_{Al} causes a distortion of the lattice shortening the Y O bond length[19]. Our work does not confirm the antisite defects associated with Y_{Al} Al_Y antisite ions, the existence of which is also considered in the literature. More detailed study is required to clarify the defects' influences on their optical characteristics to improve the ceramic application.It is hoped that additional experimental data, together with theoretical calculations, will be obtained for high-quality ceramics.

References

1. D. Kracht, M. Frede, R. Wilhelm, and C. Fallnich, Opt. Express **13**, 6212 (2005).
2. L. Jianren, M. Prabhu, X. Jianqiu, K. Ueda, H. Yagi, T. Yanagitani, and A. A. Kaminskii, Appl. Phys. Lett. **77**, 3707 (2000).
3. J. Liu, L. Ge, L. Feng, H. Jiang, H. Su, T. Zhou, J. Wang, Q. Gao, and J. Li, Chin. Opt. Lett. **14**, 051404 (2016).
4. G. Quarles, in *Proceedings of the 46th Army Sagamore Materials Research Conference* (2005).
5. R. Feldman, Y. Golan, Z. Burshtein, S. Jackle, I. Moshe, A. Meir, Y. Lumer, and Y. Shimony, Opt. Mater. **33**, 695 (2011).
6. K. Ueda, in *Proceedings of the 3rd International Conference on Ultrahigh Intensity Lasers: Development, Science and Emerging Applications* (2008).
7. Y. Shen, Y. Bo, N. Zo, Y. Go, Q. J. Peng, J. Li, Y. B. Pan, J. Y. Zhang, D. F. Cui, and Z. Y. Xu, IEEE J. Sel. Top. Quantum Electron. **21**, 1206408 (2015).
8. G. Quarles, in *Proceedings of ASSP Ceramic Lasers Summit* (2008), p. 1364.
9. A. Mandl and E. K. Klimek, in *Conference on Lasers and Electro-Optics (CLEO)* (2010), paper JThH2.
10. J. Chen and J. Li, Opt. Laser Technol. **63**, 50 (2014).
11. T. Dascalu, G. Croitoru, O. Grigore, and N. Pavel, Photon. Res. **4**, 267 (2016).
12. D. E. Zelmon, K. L. Schepler, S. Guha, D. Rush, S. M. Hegde, L. P. Gonzalez, and J. Lee, Proc. SPIE **5647**, 0277 (2005).
13. M. Sekita, H. Haneda, T. Yanagitani, and S. Shirasaki, J. Appl. Phys. **67**, 453 (1990).
14. M. Prabhu, J. Song, C. Li, J. Xu, K. Ueda, A. A. Kaminskii, H. Yagi, and T. Yanagitani, Appl. Phys. B **71**, 469 (2000).
15. Y. N. Xu and W. Y. Ching, Phys. Rev. B. **61**, 3 (2000).
16. V. V. Laguta, A. M. Slipenyuk, J. Rosa, M. Nikl, A. Vedda, K. Nejezchleb, and K. Blazek, Radiation Measurement **38**, 735 (2004).
17. R. F. Belt, J. R. Latore, R. Uhrin, and J. Paxton, Appl. Phys. Lett. **25**, 218 (1974).
18. S. Qiao, Y. Zhang, X. Shi, B. Jiang, L. Zhang, X. Cheng, L. Li, J. Wang, and L. Gui, Chin. Opt. Lett. **13**, 051602 (2015).
19. V. V. Laguta, M. Nikl, A. Vedda, E. Mihokova, J. Rosa, and K. Blazek, Phys. Rev. B **80**, 045114 (2009).